Radical damage to proteins studied by EPR spin-trapping techniques

Jean-Louis Clément,*[a] Bruce C. Gilbert,[b] Antal Rockenbauer[c] and Paul Tordo[a]

[a] *Laboratoire SREP, UMR 6517, CNRS et Université d'Aix-Marseille 1 et 3, Case 521, Av. Esc. Normandie-Niemen, 13397 Marseille cedex 20, France. E-mail: jlclement@excite.com, tordo@srepir1.univ-mrs.fr; Fax: 00 33 491 988 512; Tel: 00 33 491 288 610*

[b] *Chemistry Department, University of York, Heslington, York, UK YO10 5DD. E-mail: bcg1@york.ac.uk*

[c] *Chemical Research Center, Institute for Chemistry, H-1525, Budapest, PO Box 17, Hungary. E-mail: rocky@cric.chemres.hu*

Received (in Cambridge, UK) 6th April 2001, Accepted 18th June 2001
First published as an Advance Article on the web 6th August 2001

We report the use of the novel spin trap DEPMPO in conjunction with EPR spectroscopy to provide evidence for free-radical mediated oxidation of some proteins in aqueous solution, with systems including metal ions, peroxides or both. In addition we have used a novel approach involving detailed spectral simulation (to reproduce *anisotropic* features of phosphorus, hydrogen and nitrogen splittings) to confirm structural assignments.

Oxidation of bovine serum albumin (BSA) with either Ce^{4+} or $IrCl_6^{2-}$ leads to the predominant formation of spin-trapped oxygen-centred free-radicals, attributed to tyrosyl-based adducts, a reaction also observed for sulfur-free analogues (lysozyme and tyrosine-containing models). Similar spectra were obtained from reactions involving oxidation with HRP/H_2O_2 and methaemoglobin/H_2O_2 couples, through intermolecular oxidation of the proteins *via* oxo–iron intermediates.

Oxidation of BSA with peroxynitrite leads to an anisotropic spectrum which is assigned to the trapping of a sulfur-centred radical. This assignment has been confirmed *via* denaturation of the spin-adduct (and simulation of the resulting less immobilized spectrum). Reaction of the hydroxyl radical with BSA and lysozyme, in Fenton-type reactions, leads to the detection of anisotropic spectra derived from the spin-trapping of carbon-centred radicals, whose assignment is discussed.

Introduction

Continued extensive interest surrounds the reactions of free-radicals in biological systems, with emphasis on their formation, as a result of endogenous processes and as the consequence of externally stimulated events (radiation, photolysis and reaction of xenobiotic species), and their subsequent reactions.[1,2] There is special interest in the reactions of $O_2^{-\bullet}/HO_2^{\bullet}$ and $HO^{\bullet}$, the latter being formed from H_2O_2 (resulting from superoxide dismutation) *via* Fenton-type reactions with endogenous or exogenous metal ions. Subsequent damage to DNA, proteins and lipids has been widely explored, not least in the context of ageing, diseases and the development of drugs.[3] We have been particularly interested in potential free-radical damage to proteins which has been implicated in a number of specific diseases (including diabetes, atherosclerosis) and neurodegenerative diseases.[4] The molecular consequences of free-radical damage to proteins have been recently reviewed.[5]

The work to be described here was designed to extend the use of EPR spin-trapping techniques and the simulation of *anisotropic* EPR spectra to identify the initial targets of attack by free-radicals and different transition metal ions (which are capable of one-electron oxidation). The key principle in the spin-trapping technique is the addition of a first-formed transient free-radical ($FR^{\bullet}$) to a suitable nitrone or nitroso compound [reactions (1) and (2)] to give nitroxide (aminoxyl) radicals which are generally longer-lived and whose EPR spectra may provide information about the initial site of attack (*e.g.* to give carbon-, sulfur- or oxygen-centred radicals depending on the oxidant or the reaction).

(1)

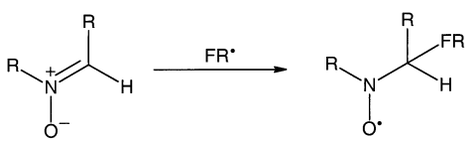

(2)

Nitrones, especially those with a cyclic structure, provide valuable information from their adducts with oxygen or sulfur radicals, largely from the variation observed in the β-hydrogen coupling constant as a result of conformational preferences (see below). The spin-trapping of proteinyl-radicals leads generally to immobilised or slowly tumbling spin-adducts exhibiting EPR anisotropic spectra which are dramatically dependent on the initial protein and the spin trap itself.[6,7] Unambiguous assignment of the spectrum is not usually possible due to the broad nature of the EPR signal. So, definitive identification must be achieved by the design of ancillary experiments, which are not without drawbacks, or by effecting denaturing or digestion on the proteinyl spin-adduct. Unfortunately, these processes may result in the destruction of the EPR signal and can lead to the formation of new spin-adducts, thus leading to potential misinterpretations.[8] Further information is in principle also provided by the anisotropy of the adducts' spectra. This anisotropy characterizes the motional properties of the nitroxides and hence also of the macromolecule carriers. For example, the

DOI: 10.1039/b103211a

occurrence of fragmentation and/or denaturation can be probed.[6,9]

Our experiments have largely employed the novel spin trap 5-diethoxyphosphoryl-5-methyl-1-pyrroline *N*-oxide, DEPMPO (**1**)[10] which has a β-phosphorus substituent, as well as the more widely used 5,5-dimethyl-1-pyrroline *N*-oxide, DMPO (**2**). For both types, the adducts of different types of

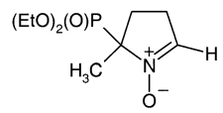

DEPMPO 1

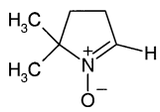

DMPO 2

radical have characteristically different β-proton splittings, in the ranges <1.5 mT (O), 1.4–1.8 mT (S) and >2.0 mT (C).[9] The extra information potentially available for the former trap, notably from the phosphorus coupling constant (and its anisotropy), and the suggestion that the phosphorylated version gives more biocompatible and longer-lived spin-adducts,[7] are potential advantages we wished to explore. Our approach has also involved the utilisation of a spectrum simulation program designed for matching anisotropic spectra of slowly tumbling macro-radicals.[11,12]

The proteins employed include BSA,[13] which possesses a free cysteine residue at position 34, and a number of chemically modified ('blocked') derivatives, and also lysozyme,[14] chosen for its lack of a free sulfhydryl group. Various oxidants have been chosen to react with these proteins in the presence of spin traps, including HRP/H_2O_2 (horse radish peroxidase), Met/H_2O_2 (methaemoglobin) and peroxynitrite ($HOON{=}O/^{-}OON{=}O$, $pK_a = 6.9$) as well as metal ions (Ce^{4+} and Ir^{4+}) and redox couples Fe^{2+}/H_2O_2 (to give $HO^{\bullet}$) and $Ti^{3+}/S_2O_8^{2-}$ (to give $SO_4^{-\bullet}$).

Experimental

Chemicals

Horse radish peroxidase (HRP), pig methaemoglobin (Met), myoglobin (Myo) from horse heart, bovine serum albumin (BSA), bovine serum albumin-S-cysteinyl (thiol-blocked BSA), lysozyme (lys), poly(gly-tyr) and DMPO were purchased from Sigma and used as supplied, with the exception of DMPO which was purified by vacuum distillation before use. DEPMPO was synthesised as described previously.[15] All solutions were prepared in 100 mM phosphate buffer at pH 7.0, using high-purity deionised water with the exception of Fe(II)–ethylenediaminetetraacetic acid (EDTA) and Ce(IV)–nitrilotriacetic acid (NTA), which were made up only in high-purity deionised water. Peroxynitrite (pN) was synthesised as described previously.[16]

Protein modification

Protein modifications were carried out using previously described methods.[17] Thiol-blocked BSA was synthesised by mixing BSA (90 mg, 1 ml high-purity deionised water) with *N*-ethylmaleimide (NEM) (16.8 mg, 0.6 ml high-purity deionised water) for 10 minutes. The solution was passed through a G-25 Sephadex column and eluted with high-purity deionised water. The remaining protein solution was freeze dried. The loss of the thiol group was determined by the DTBN assay.[18]

Tyrosyl modifications of BSA and lysozyme were achieved by reaction of the protein with *N*-acetylimidazole (NAI). Typically, protein (100 mg, 4 ml high-purity deionised water) was mixed with NAI (100 eq., 1.5 ml high-purity deionised water). The reaction was allowed to stand until there was no decrease in the absorption at 278 nm. The mixture was purified by passing through a Sephadex G-25 column and eluted with high-purity deionised water. The remaining protein solution was freeze dried.

EPR spectroscopy

EPR measurements were carried out on Bruker ESP 300 and EMX spectrometers (both X-band) at room temperature except where stated otherwise. Samples were recorded using a quartz aqueous-solution flat-cell. Typical spectrometer settings are given in the relevant figure legends. The spin-trap concentrations (given in the text and figure legends) were typically in the range 5–100 mM and oxidant concentrations 1–25 mM.

EPR simulations

The EPR simulation program employed[11,12] describes the effect of slow tumbling by using effective tensorial elements for Zeeman and hyperfine interactions, with an orientation-dependent line-width tensor. The principal axes of interactions (namely the g, A_N, A_H and A_P tensors) are assumed to be parallel. In the case of the DMPO adducts, six spin-Hamiltonian parameters were adjusted ($g_{//}$, $g_{\perp}$, $A_{N//}$, $A_{N\perp}$, $A_{H//}$, $A_{H\perp}$), while for DEPMPO the total was eight (to include $A_{P//}$ and $A_{P\perp}$).

Residual motion in slowly tumbling radical-adducts can modify anisotropic spectra, as compared to spectra recorded in frozen solution (typically the parallel components are broadened and shifted with the largest variation in the high field region); the effect of slow and anisotropic tumbling motion was taken into account by introduction of a hyperfine dependent linewidth tensor [eqns. (3) and (4)], where M_N is the magnetic

$$W_{//}^2 = a_{//} + \beta_{//}M_N + \gamma_{//}M_N^2 \quad (3)$$

$$W_{\perp}^2 = a_{\perp} + \beta_{\perp}M_N + \gamma_{\perp}M_N^2 \quad (4)$$

quantum number for nitrogen and where axial symmetry is assumed. The orientation dependence is given by eqn. (5),

$$W^2(\theta) = W_{\perp}^2\sin^2\theta + W_{//}^2\cos^2\theta \quad (5)$$

which is formally analogous to the expression that is used to describe the broadening *via* strain effects.[19] To limit the number of linewidth parameters, we replaced the $\beta_{//}$, $\beta_{\perp}$, $\gamma_{//}$ and $\gamma_{\perp}$ tensor elements by isotropic constants β and γ and adjusted these in the curve-fitting procedure. We considered the lineshape function as a weighted mixture of Lorentzian and Gaussian curve (for solution spectra, the lineshapes were largely Lorentzian; in the solid-state a Gaussian shape predominated). All tensorial elements were adjusted by combining iteration and least squares procedures, with a search for the minimum square deviation between experimental and computed spectra.

For each spectrum simulation reported, we also started from different but realistic parameter sets and the iteration converged to the same (optimum) values. Iterations trapped in local minima (which were rejected) were recognised by the significantly larger least squares error.

Results and discussion

Simulation of EPR spectra obtained with haem-proteins

The haem-protein family (including myoglobin or haemoglobin) can exhibit a pseudo peroxidase activity: on reaction with H_2O_2, they are believed to form a reactive ferryl-oxo haem intermediate [iron(IV)–oxo porphyrin radical-cation][20,21] able to oxidise different biomolecules and hence contribute to cell degradation.[2,5] Haem-proteins, such as horse radish peroxidase (HRP) have consequently been used in this work in an attempt

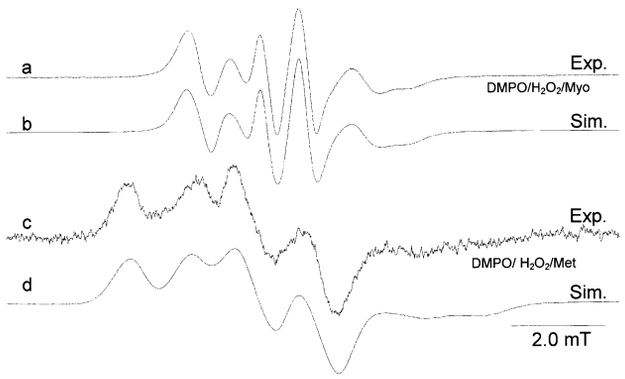

Fig. 1 (a) EPR spectrum of the myoglobin-derived radical adduct formed in the reaction of myoglobin with H_2O_2 in the presence of DMPO, (b) simulated spectrum, (c) EPR spectrum of the methaemoglobin-derived radical adduct formed in the reaction of methaemoglobin with H_2O_2 in the presence of DMPO, (d) simulated spectrum (for parameters see Table 1). Concentration: (a) and (c) DMPO 100 mM, (a) myoglobin 4 mM, H_2O_2 4 mM, (c) methaemoglobin 4 mM, H_2O_2 4 mM. Setting (a): modulation amplitude 0.1 mT, time constant 163.8 ms, sweep time 83.9 s, gain 2×10^4, microwave power 50 mW. Setting (c): modulation amplitude 0.25 mT, time constant 163.8 ms, sweep time 83.9 s, gain 1×10^5, microwave power 50 mW.

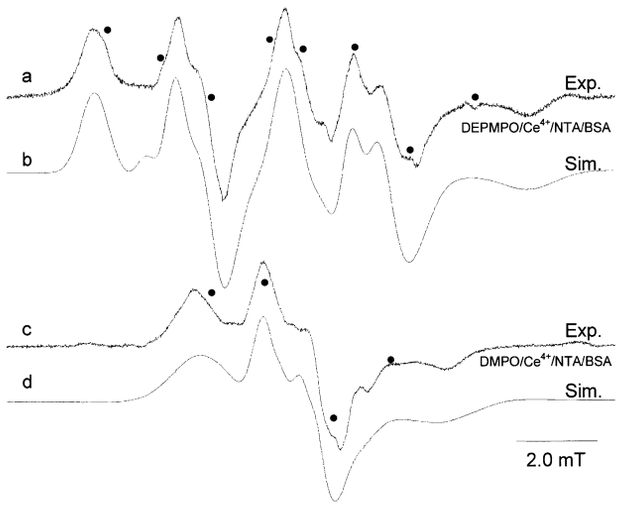

Fig. 2 (a) EPR spectrum of an oxygen-centred BSA-derived radical adduct formed in reaction of BSA with Ce^{4+}/NTA in presence of DEPMPO, (b) simulated spectrum, (c) EPR spectrum of an oxygen-centred BSA-derived radical adduct formed in the reaction of BSA with Ce^{4+}/NTA in the presence of DMPO, (d) simulated spectrum. The low intensity peaks indicated (•) are attributed to the hydroxyl-radical adduct (for parameters see Table 1). Concentration: (a) DEPMPO 5 mM, (c) DMPO 5 mM, BSA 1.5 mM, Ce^{4+}/NTA 5/10 mM. Setting (a) and (c): modulation amplitude 0.2 mT, time constant 20.48 ms, sweep time 1342.1 s, gain 10^5, microwave power 20 mW.

to characterize radical damage to proteins: our aim in initially studying these proteins, which are known to produce anisotropic spectra in the presence of spin traps, was to demonstrate that the effective simulation of anisotropic spectra is now possible.

The reaction of H_2O_2 (4 mM) with myoglobin (4 mM) in the presence of DMPO (typically *ca.* 100 mM) led to the detection of a spectrum characteristic of a partially immobilised spin-adduct (see *e.g.* Fig. 1a); previous experiments with blocked derivatives suggest that this spectrum is the result of the spin-trapping of an oxygen-centred radical hence assigned to a tyrosyl-based adduct (*i.e.* from a phenoxyl radical derived from tyrosine).[8,20,21] On the other hand the reaction of hydrogen peroxide with haemoglobin (in the presence of DMPO) (Fig. 1c) clearly led to a different adduct assigned to a sulfur-centred spin-adduct, again as previously noted.[22,23] The spectra obtained are anisotropic and it is not possible to analyse or attribute them easily. However, optimised simulations of these spectra have now been computed with the approach described above (see refs. 11 and 12), taking into account the anisotropy of the nitrogen and hydrogen splittings (the latter of which is of course less significant). As can be seen from Fig. 1b and 1d, very good agreement is obtained on the basis of simulation for a single (dominant) species; the extent of anisotropy evidently increases (as measured by the increase of the calculated values of $A_{//} - A_{\perp}$) with the size of the protein (results given in Table 1) so that, as expected, there is a greater extent of motional averaging (lower $A_{//}$, $A_{\perp}$) for the smaller, more rapidly tumbling molecule. The splittings derived from these simulations, notably the average values, are very characteristic of the individual spin-adducts and the values of the hydrogen coupling constants allow clear cut conclusions to be drawn, though the absolute magnitudes of hydrogen splittings show some divergence: this is not unexpected given the conformational dependence of the spectra and the possibility that other spectra underlie the major component. Particularly notable in these examples are the average values of the hydrogen splittings of the DMPO adducts from myoglobin and methaemoglobin ($\langle a_H \rangle = 0.80$ and 1.22 mT, respectively), which are clearly characteristic of oxygen- and sulfur-centred species, respectively. We believe that this confirms the original assignments. Comparable results, with an additional splitting from phosphorus, were obtained with DEPMPO (see Table 1). The approach was next employed in studies of a range of oxidants and substrates from which broadened anisotropic spectra might be anticipated.

Reaction of BSA, its derivatives and lysozyme with Ce^{4+}

i) Initial experiments involved the use of DEPMPO, Ce^{4+}/NTA and BSA in aqueous solution at pH 7, over a range of concentration of trap and oxidant (see above). In experiments with relatively low trap concentrations (5 mM) and with [Ce^{4+}] 5–25 mM, and with the metal ion added last, a strong and relatively long-lived EPR signal was detected (see Fig. 2a). This spectrum consists of an anisotropic nitrogen splitting as well as a small hydrogen splitting, further split by a large phosphorus splitting. The corresponding spectrum obtained with DMPO is shown in Fig. 2c. Spectral simulations were carried out (Fig. 2b and 2d) with the program developed to include the anisotropy of the nitrogen as well as those of phosphorus and hydrogen; in each case, a very good fit was obtained for a single species, with the parameters shown in Table 1. In particular, it is encouraging that this automatic simulation for β-phosphorylated nitroxide spin-adducts gives parameters (including those for phosphorus) close to those identified (using a similar procedure) by Tordo and Chachaty and co-workers in the calculation of low temperature spectra of β-phosphorylated nitroxides in glycerol.[24] It is notable that the magnitude of the resulting average hydrogen splitting in some cases is somewhat less than the apparent splitting measured directly from the anisotropic spectrum.

We believe that the mechanism of reaction involves "authentic" spin-trapping of free-radicals, but we need to exclude two alternative mechanisms for nitroxide formation. The first consists of the nucleophilic addition of the protein to the trap followed by oxidation by Ce^{4+} of the corresponding hydroxylamine to the observed nitroxide. Similar experiments in the absence of Ce^{4+} but in the presence of $K_3Fe(CN)_6$, which is known to oxidise first-formed hydroxylamines (and which was added 3 hours after the protein), led to an EPR-silent spectrum. We hence conclude that this mechanism is unlikely. The second possible mechanism involves oxidation of the spin trap itself by Ce^{4+} to the nitrone radical-cation followed by the addition of protein. If this reaction occurs, we believe that the most

Table 1 Simulated parameters of EPR spectra of spin-adduct proteins obtained in the presence of spin trap at pH = 7.0

Protein/reactant	Spin trap	Hyperfine splitting constant/mT [a]									Adduct type
		$A_{//}$	$A_{\perp}$	$\langle a_N \rangle$	$A_{//}$	$A_{\perp}$	$\langle a_H \rangle$	$A_{//}$	$A_{\perp}$	$\langle a_P \rangle$	
Myo/H_2O_2	DEPMPO	2.01	1.08	1.39	0.77	0.89	0.80	4.62	4.36	4.46	O
Met/H_2O_2	DEPMPO	2.71	0.88	1.49	1.39	1.40	1.40	5.09	4.47	4.68	S
Myo/H_2O_2	DMPO	1.98	1.16	1.43	0.77	0.82	0.80				O
Met/H_2O_2	DMPO	2.87	0.49	1.28	1.17	1.25	1.22				S
BSA/Ce^{4+}/NTA	DEPMPO	2.89	0.55	1.33	0.31	0.65	0.53	4.79	4.31	4.47	O
Lys/Ce^{4+}/NTA	DEPMPO	2.06	1.10	1.42	0.81	0.95	0.90	5.02	4.51	4.68	O
BSA/Ce^{4+}/NTA	DMPO	2.55	0.78	1.37	0.84	0.88	0.86				O
BSA/Ce^{4+}/NTA/guanidine, HCl	DEPMPO	1.85	1.31	1.49	1.19	1.43	1.35	4.97	4.47	4.64	S
BSA/peroxynitrite	DEPMPO	2.64	0.97	1.53	1.53	1.85	1.74	6.09	3.75	4.52	S
BSA/peroxynitrite	DMPO	2.67	0.82	1.44	1.15	1.27	1.23				S
BSA/peroxynitrite/guanidine, HCl	DEPMPO	1.58	1.34	1.42	1.28	1.49	1.42	4.87	4.43	4.57	S
BSA/H_2O_2/Fe^{2+}/EDTA	DEPMPO	2.87	1.13	1.70	2.00	2.12	2.08	5.22	4.60	4.80	C
BSA/$Na_2S_2O_8$/$Ti_2(SO_4)_3$/EDTA	DEPMPO	2.73	0.75	1.41	1.67	1.94	1.76	5.26	4.48	4.74	C
BSA/H_2O_2/Fe^{2+}/EDTA	DMPO	3.20	1.17	1.85	2.23	2.32	2.26				C
BSA/$Na_2S_2O_8$/$Ti_2(SO_4)_3$/EDTA	DMPO	3.30	0.95	1.73	2.16	2.20	2.17				C
Lys/H_2O_2/Fe^{2+}/EDTA	DEPMPO	1.70	1.39	1.49	1.96	2.08	2.04	5.18	4.54	4.75	C
BSA/H_2O_2/Fe^{2+}/EDTA/urea	DEPMPO	1.65	1.39	1.47	1.90	2.21	2.00	5.07	4.47	4.87	C
BSA/H_2O_2/Fe^{2+}/EDTA/urea	DMPO	1.69	1.47	1.54	2.11	2.34	2.26				C

[a] Typical g-values from simulation were $g_{//}$ 2.006, $g_{\perp}$ 2.008.

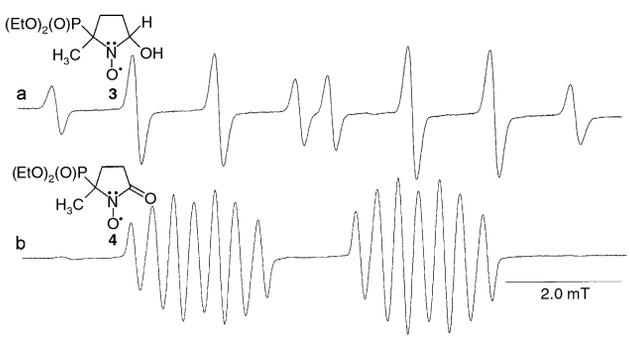

Fig. 3 (a) EPR spectrum of hydroxyl-radical adduct formed in the reaction of H_2O_2 with Fe^{2+}/EDTA in the presence of DEPMPO, (b) EPR spectrum of DEPMPOX formed in the reaction of DEPMPO with Ce^{4+}/NTA. Concentration: (a) DEPMPO 50 mM, H_2O_2 2.0 mM, Fe^{2+}/EDTA 2.0 mM. (b) DEPMPO 50 mM, Ce^{4+}/NTA 0.5 mM. Setting (a) and (b): modulation amplitude 0.15 mT, time constant 40.2 ms, sweep time 83.3 s, gain 8×10^4, microwave power 20 mW.

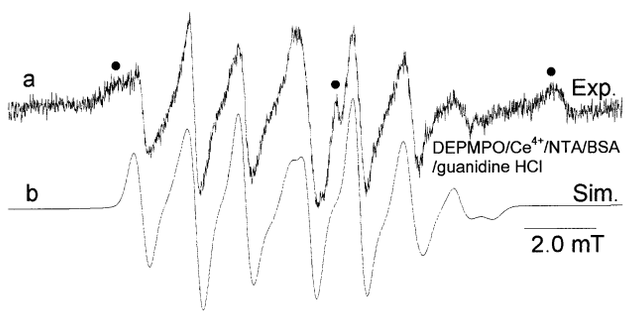

Fig. 4 (a) EPR spectrum of the sulfur-centred BSA-derived radical adduct formed in reaction of BSA with Ce^{4+}/NTA in the presence of DEPMPO after denaturation with guanidine hydrochloride (4 M), (b) simulated spectrum. The spectrum indicated (•) is attributed to glass peaks (for parameters see Table 1). Concentration: DEPMPO 5 mM, BSA 1.5 mM, Ce^{4+}/NTA 5/10 mM, guanidine hydrochloride (4 M). Setting: modulation amplitude 0.25 mT, time constant 20.48 ms, sweep time 83.9 s, gain 10^5, 10 scans, microwave power 20 mW.

important nucleophile, water, would have added preferentially, leading to the formation of the hydroxyl adduct and DEPMPOX (**4**) as obtained in absence of protein (see below).

Variation of the Ce^{4+} concentration from 5 to 25 mM was found to lead to a steady increase in the spectrum intensity (as expected from an increase in the rate of the oxidation reaction as [Ce^{4+}] is increased). However, increasing cerium concentration also led ultimately to the appearance of an extra EPR signal from the HO$^{\bullet}$ spin-adduct (**3**), especially at high trap concentrations, probably formed by reaction of the trap with Ce^{4+} [although the reaction of Ce^{4+} (0.5 mM) alone with either of the spin traps in the absence of protein led to a strong signal interpreted in each case as the oxidised form of the spin trap (DMPOX $a_N = 0.71$, $a_H = 0.42$ mT and DEPMPOX $a_N = 0.78$, $a_H = 0.41$, $a_P = 4.12$ mT)][15,25] with only a small amount of hydroxyl spin-adduct (see Fig. 3).

At this stage, and from the small β-H coupling constants obtained from experiments with DEPMPO and DMPO (typically DMPO: $\langle a_H \rangle = 0.86$ mT; DEPMPO: $\langle a_H \rangle = 0.53$ mT), we conclude that an *oxygen-centred radical* has been trapped after reaction of BSA with Ce^{4+}. In the absence of oxygen, removed by freeze–pump–thaw cycle, the spectrum obtained with DEPMPO was found to be the same as under normoxic conditions, but with a small increase in the spectrum intensity, an observation which excludes the spin-trapping of a protein-derived peroxyl radical. These findings, especially the remarkably low β-H value for the DEPMPO adduct (discussed in more detail later), strongly suggest the reassignment of the spectra from DMPO (dominated by a relatively small doublet) previously reported by us[7,9] and interpreted as a thiyl radical. A thiyl radical would be expected to have a somewhat larger coupling; support for this expectation is described below. It should be noted, of course, that a minor contribution from such a species could not be ruled out.

In complete contrast to the results of experiments shown in Fig. 2, when the EPR spectra were recorded in experiments with protein which had been denatured (with urea 8 M or guanidine hydrochloride 4 M) *after* reaction with Ce^{4+}, a very different spectrum of a less immobilized spin-adduct was obtained (as the anisotropic spectrum disappeared) characterised by a decrease of $A_{//} - A_{\perp}$ (Fig. 4). The following parameters $\langle a_N \rangle = 1.49$, $\langle a_H \rangle = 1.35$, $\langle a_P \rangle = 4.64$ mT strongly suggest that a sulfur-centred radical has been trapped under these conditions.

The following experiments were performed to attempt to confirm and rationalise this behaviour.

ii) Experiments carried out with the S-blocked BSA derivatives, BSA-S-NEM and BSA-S-cysteinyl, gave results (data not shown) closely similar to those obtained with BSA itself, which strongly suggest that the oxidised species trapped with native BSA, is not sulfur-centred. This implies also that the sulfur group is probably not the initial target of attack by cerium, followed by radical transfer to another residue (though,

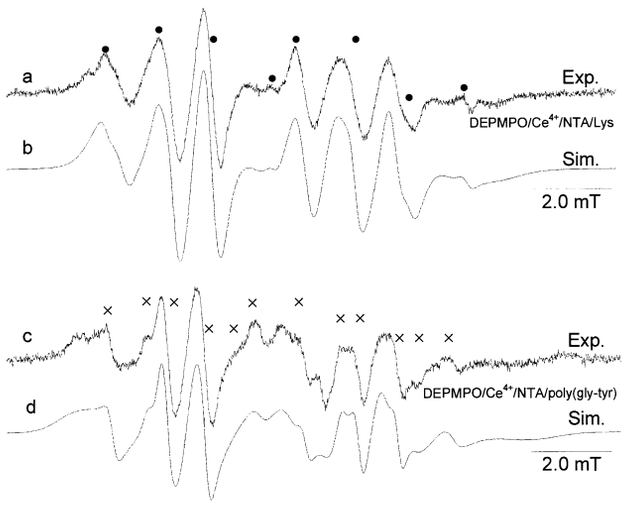

Fig. 5 (a) EPR spectrum of oxygen-centred lysozyme-derived radical adduct formed in the reaction of lysozyme with Ce^{4+}/NTA in the presence of DEPMPO, (b) simulated spectrum, (c) EPR spectrum of the oxygen-centred poly(gly-tyr)-derived radical adduct formed in the reaction of poly(gly-tyr) with Ce^{4+}/NTA in the presence of DEPMPO, (d) simulated spectrum. The spectrum indicated (×) is attributed to a smaller tyrosyl-derived fragment radical. The spectrum indicated (•) is attributed to the hydroxyl radical adduct (for parameters see Table 1). Concentration: (a) DEPMPO 10 mM, lysozyme 3.0 mM, Ce^{4+}/NTA 5/10 mM. Setting (a): modulation amplitude 0.25 mT, time constant 163.8 ms, sweep time 671.1 s, gain 10^5, microwave power 50 mW. Concentration: (c) DEPMPO 10 mM, poly(gly-tyr) 21 mg ml^{-1}, Ce^{4+}/NTA 5/10 mM. Setting (c): modulation amplitude 0.25 mT, time constant 40.9 ms, sweep time 83.9 s, gain 5×10^5, microwave power 50 mW.

as noted, we cannot exclude the possibility that a small proportion of a sulfur-centred spin-adduct is present at the same time as the oxygen-centred spin-adduct in experiments with native BSA, Ce^{4+} and DEPMPO). On the other hand, denaturation of these S-blocked BSA samples after addition of Ce^{4+} and spin-trapping gave no detectable signal, unlike experiments with BSA itself for which a thiyl adduct was detected. Our experiments suggest that the thiyl spin-adduct detected after denaturation in the earlier experiment indeed reflects the oxidation of the thiyl group by Ce^{4+}. The thiyl residue, which was previously buried[13] in the native protein, evidently becomes accessible on denaturation and reacts with the remaining Ce^{4+}.

iii) When similar experiments were carried out with Ce^{4+} and glutathione in the presence of DEPMPO a strong isotropic signal was detected with parameters $a_N = 1.42$, $a_H = 1.42$, $a_P = 4.58$ mT, characteristic of a thiyl adduct (data not shown), as might be expected from the well-known ability of Ce^{4+} to oxidise the -SH function.[26,27]

iv) On the other hand, reaction of Ce^{4+} under similar conditions with lysozyme (Fig. 5a), which has no thiyl residue, led to the detection of a strong spectrum characteristic of an oxygen-centred trapped radical, simulated (Fig. 5b) with parameters indicated in Table 1.

v) Additionally the reaction of poly(gly-tyr) with Ce^{4+} (Fig. 5c) in the presence of DEPMPO also led to the detection of a spectrum virtually identical to those detected for lysozyme and Ce^{4+}, as would be expected if oxidation has occurred at tyrosine moieties.

On the basis of the observations noted above we conclude that Ce^{4+} reacts with BSA by oxidation preferentially to give an oxygen-centred species which we suggest is a tyrosyl-based residue. Spin-adducts of tyrosyl-derived radicals have been previously reported (*cf.* ref. 21). For example, a spectrum at 77 K of the myoglobin spin-adduct obtained with DMPO after reaction with H_2O_2, shows similar features to the spectrum obtained here with BSA and Ce^{4+} in the presence of DMPO at 193 K (data not shown).[28] Further support for our assertion comes firstly from the finding that when the tyrosine residues are blocked (see Experimental section) the signal intensities are dramatically reduced. It is notable that when tyrosine residues are blocked, significant damage does not appear to occur at the sulfur moiety as might have been expected.

Reaction of other oxidants with BSA and lysozyme

The characteristic features of the spectra obtained for BSA and lysozyme with Ce^{4+} were also obtained when reactions were carried out with[20] K_2IrCl_6 (typically with concentrations of DEPMPO 10.0 mM; BSA 1.5 mM; K_2IrCl_6 10.0 mM) and in experiments involving HRP/H_2O_2 or Met/H_2O_2 (DEPMPO 10.0 mM; BSA 1.5 mM; H_2O_2 1.0 mM and HRP (220 u mg^{-1}) 18.0 mg ml^{-1} or Met 1.5 mg ml^{-1}). In the second set of experiments it is believed that a ferryl-oxo haem species is responsible for the oxidation. Under the conditions we employed there was no evidence for these signals in the HRP/H_2O_2 system without the addition of BSA or lysozyme, so we believe that intermolecular radical damage has occurred; this observation provides further support for the claim that radical transfer occurs between HRP/H_2O_2 and the tyrosyl residue of BSA.[29] The similarity of spectra obtained both with Ce^{4+} and the HRP/H_2O_2 system implies that the same tyrosine-derived radicals have been trapped. This hypothesis was confirmed by the decrease of signal intensity when EPR experiments were carried out with tyr-blocked BSA, both with Ce^{4+} and HRP/H_2O_2. Given the apparent ease of spin-trapping of the proteinyl-derived radical in experiments with HRP, we conclude that the tyrosyl radicals are formed on the surface of the protein rather than on buried residues.

Reaction of peroxynitrite with BSA and lysozyme: effective generation of thiyl radicals

It has been shown that in aqueous solution peroxynitrite (O=NOOH/O=NOO$^-$, pK_a = 6.9) reacts with thiols to generate thiyl radicals.[30] We have utilised EPR spin-trapping and explored the reaction of peroxynitrite with a number of proteins in water at pH = 7.0 in an attempt to generate authentic sulfur-centred radical adducts, to confirm our earlier experiments and to contrast potential routes with those observed for the metal ions.

Reactions of peroxynitrite and BSA in the presence of DEPMPO at pH = 7.0 led to the detection of an anisotropic spectrum, simulated with a set of parameters which leads to $\langle a_N \rangle$ 1.53, $\langle a_H \rangle$ 1.74 and $\langle a_P \rangle$ 4.52 mT attributed to a sulfur-centred adduct (Fig. 6a). On denaturation with guanidine hydrochloride a strong signal from a less immobilized sulfur-centred adduct ($a_N = 1.42$, $a_H = 1.42$, $a_P = 4.57$ mT) was obtained (Fig. 7) [with a significant decrease in $(A_{//} - A_{\perp})$]. Since the lifetime of peroxynitrite in water at pH = 7.0 is very short (typically $t_{1/2}$ = 1 s at pH = 7.4),[31] we believe that the spectrum obtained after denaturation is from the trapping of the thiyl radical formed in the initial oxidation. Simulation of both spectra (Fig. 6b and Fig. 7b) shows very good agreement and confirms the assignment of these spectra to sulfur-centred trapped radicals [though with evident conformational differences reflected in the slightly different a(β-H) values]. No signal was detected with S-blocked BSA (with BSA-S-cysteinyl, BSA-S-NEM or lysozyme as expected on this basis).

We have also investigated the reaction of peroxynitrite with BSA in the presence of DMPO and obtained further evidence for the spin-trapping of a sulfur-centred proteinyl-derived species (Fig. 6d and 6e).

Reaction of the hydroxyl radical with BSA and lysozyme

Reaction of BSA with HO$^•$ (generated from Fe^{2+}/EDTA and H_2O_2) in the presence of DEPMPO in water at pH 7.0 led to the detection of a strong anisotropic EPR spectrum dominated by a component with a large β-hydrogen splitting ($\langle a_H \rangle$ 2.08 mT),

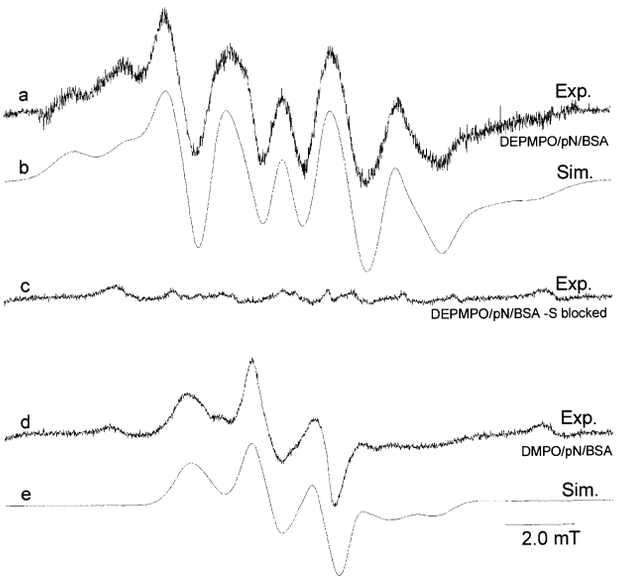

Fig. 6 (a) EPR spectrum of the sulfur-centred BSA-derived radical adduct formed in reaction of BSA with ONOOH/$ONOO^-$ in the presence of DEPMPO, (b) simulated spectrum, (c) S-blocked BSA, (d) EPR spectrum of sulfur-centred BSA-derived radical adduct formed in the reaction of BSA with ONOOH/$ONOO^-$ in the presence of DMPO, (e) simulated spectrum (for parameters see Table 1). Concentration: (a) DEPMPO 100 mM, (d) DMPO 100 mM, (a) and (d) BSA 1.5 mM, (c) S-blocked BSA 1.5 mM, (a) (c) and (d) peroxynitrite 2.0 mM. Setting (a) (c) and (d): modulation amplitude 0.25 mT, time constant 20.5 ms, sweep time 1342.2 s, gain 10^5, microwave power 20 mW.

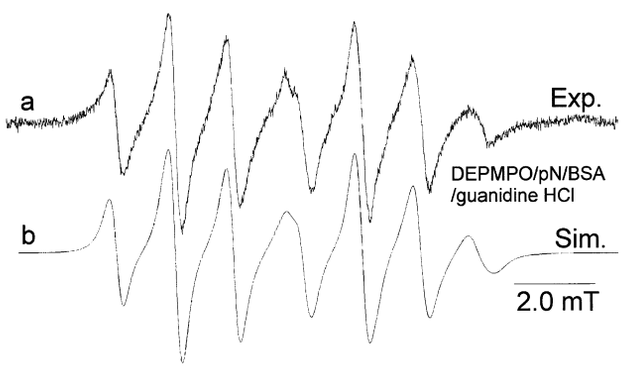

Fig. 7 (a) EPR spectrum of the sulfur-centred BSA-derived radical adduct formed in the reaction of BSA with ONOOH/$ONOO^-$ in the presence of DEPMPO, after denaturation with guanidine hydrochloride (4 M), (b) simulated spectrum (for parameters see Table 1). Concentration: DEPMPO 100 mM, BSA 1.5 mM, peroxynitrite 2.0 mM, guanidine hydrochloride 4 M. Setting: modulation amplitude 0.25 mT, time constant 20.48 ms, sweep time 83.9 s, gain 10^5, microwave power 20 mW.

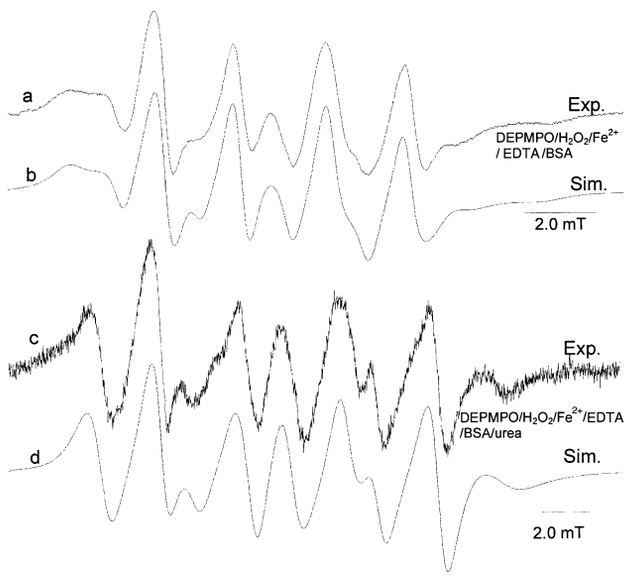

Fig. 8 (a) EPR spectrum of the carbon-centred BSA-derived radical adduct formed in the reaction of BSA with Fe^{2+}/EDTA/H_2O_2 in the presence of DEPMPO, (b) simulated spectrum, (c) EPR spectrum of the carbon-centred BSA-derived radical adduct formed in the reaction of BSA with Fe^{2+}/EDTA/H_2O_2 in the presence of DEPMPO after denaturation with urea (9 M), (d) simulated spectrum (for parameters see Table 1). Concentration: (a) (c) DEPMPO 2.5 mM, BSA 2.25 mM, Fe^{2+}/EDTA 2.0 mM, H_2O_2 2.0 mM, (c) urea (9 M). Setting: modulation amplitude 0.25 mT, time constant 20.48 ms, sweep time 335.5 s, (c) sweep time 83.9 s, gain 3.17×10^5, microwave power 20 mW.

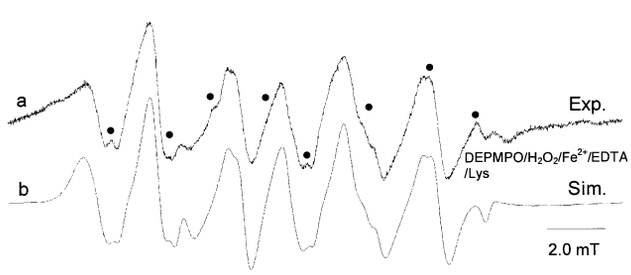

Fig. 9 (a) EPR spectrum of the carbon-centred lysozyme-derived radical adduct formed in the reaction of lysozyme with Fe^{2+}/EDTA/H_2O_2 in the presence of DEPMPO, (b) simulated spectrum. The weak signals indicated (•) are attributed to the hydroxyl-radical adduct (for parameters see Table 1). Concentration: DEPMPO 2.5 mM, lysozyme 4.9 mM, Fe^{2+}/EDTA 2.0 mM, H_2O_2 2.0 mM. Setting: modulation amplitude 0.25 mT, time constant 20.48 ms, sweep time 335.5 s, gain 3.17×10^5, microwave power 20 mW.

attributed to a carbon-centred radical adduct (Fig. 8a): denaturation with urea led to the detection of an analogous spectrum characteristic of a less immobilised spin-adduct (Fig. 8c) distinguished by a decrease of $A_{//} - A_{\perp}$. The high value of $\langle a_N \rangle$ in the anisotropic spectrum is notable and will be discussed further below. Closely similar spectra to these were observed for reaction of $HO^{\bullet}$ with lysozyme in presence of DEPMPO, without denaturation (Fig. 9). With DMPO analogous spectra were obtained (*e.g.* Fig. 10a). The spectrum obtained after reaction of BSA with the sulfate radical-anion ($SO_4^{-\bullet}$) (Fig. 10c) also shows the formation of a carbon-centred radical adduct. Nevertheless, one can note that the EPR signals are different: this is presumably explained by a different selectivity of the attacking radicals leading to different carbon-centred radicals on BSA. Experiments with direct observation (flow, Ti^{3+}/EDTA/H_2O_2, BSA) led to complex spectra in which carbon-centred species of the type $-CH_2-{}^{\bullet}CH-COO^-$ can be detected.[32] We believe that these are the species trapped in these experiments. It is notable that hydrogen abstraction from C–H bonds is evidently highly competitive with reaction of S–H (dominant in GSH).

The large average nitrogen coupling for the carbon-centred radical-adduct obtained with BSA (though not after denaturation or for lysozyme) is notable: one possible explanation is pyramidalization at the nitroxide nitrogen induced by steric effects. A second possibility is that the principal direction for *g* and splitting tensors are not necessarily parallel and/or that the rotational tumbling is anisotropic. In these conditions the isotropic average of splitting may significantly deviate from the arithmetic average of principal values. Furthermore, when the motion is not rapid the adjusted 'effective' $A_{N//}$ can be smaller, and $A_{N\perp}$ larger than the frozen solution value, which may give an $\langle A_N \rangle$ different from the isotropic value.

We also note the relatively low a(β-H) value for some carbon-centred radical adduct(s) of DEPMPO (*ca.* 2.0 mT). We suggest that, for example, for a bulky spin adduct it is likely that spectra are detected with a predominant (or exclusive) preferred conformation with the five-membered cycle pseudo-rotation frozen. This should be most marked at low temperature, which

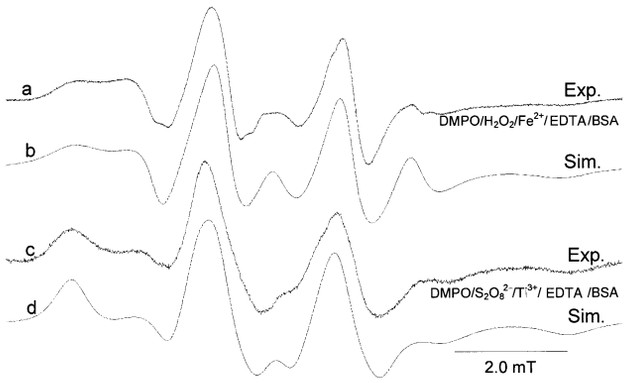

Fig. 10 (a) EPR spectrum of the carbon-centred BSA-derived radical adduct formed in the reaction of BSA with Fe^{2+}/EDTA/H_2O_2 in the presence of DMPO, (b) simulated spectrum, (c) EPR spectrum of the carbon-centred BSA-derived radical adduct formed in the reaction of BSA with $S_2O_8^{2-}$/Ti^{3+}/EDTA in the presence of DMPO, (d) simulated spectrum (for parameters see Table 1). Concentration: (a) DMPO 5 mM, (c) DMPO 20 mM, BSA 1.5 mM, (a) Fe^{2+}/EDTA 2.0 mM, H_2O_2 2.0 mM, (c) $K_2S_2O_8$ 10.0 mM, EDTA 4.0 mM, $Ti_2(SO_4)_3$ 4.0 mM. Setting (a): modulation amplitude 0.25 mT, time constant 20.48 ms, sweep time 671.1 s, gain 3.17×10^5, microwave power 20 mW. Setting (c): modulation amplitude 0.25 mT, time constant 41.0 ms, sweep time 671.1 s, gain 2×10^5, microwave power 20 mW.

led us to study some systems at −100 °C. For example, the spectrum obtained for BSA carbon-centred spin adducts of DEPMPO at low temperature, with $\langle a_H \rangle = 1.37$ and $\langle a_P \rangle = 5.20$ mT, was found to be characteristic of adducts of DEPMPO with the five-membered cycle adopting an envelope conformation [*cf.* $\langle a_H \rangle = 1.39$, $\langle a_P \rangle = 5.12$ mT calculated for the envelope conformation (^{3}E) of the DEPMPO/$^{\bullet}CH_3$ spin adduct].[33]

We also note the particularly low values of *a*(β-H) for some oxygen-centred adducts (*e.g.* 0.53 mT for BSA/Ce^{4+}/DEPMPO) compared to well-known and slightly higher isotropic constants previously reported. We suggest again that, for a bulky spin-adduct under these conditions, it is likely that spectra are detected with a predominant (or locked) preferred conformation.

Conclusion

The new approach described provides an extra valuable tool for identification of the predominant site of free-radical or metal-ion attack on macromolecules. Thus, the EPR spin-trapping technique can be significantly improved if the use of cyclic nitrones (DMPO and DEPMPO) is coupled with the use of spectrum simulation software which takes into account the motional restriction of the major spin-adduct obtained. This gives much greater confidence in spectrum analysis, and the calculated average β-proton splittings allow more confident distinction to be made between the trapping of oxygen- or sulfur- and carbon-centred species. Further, with the DEPMPO spin-adducts, the phosphorus splitting also depends on the nature of the trapped radical, affording a greater reliability for the assignment. This work is now being extended to the characterisation of peroxyl-radicals generated from macromolecules and to simulate spectra of a mixture of radicals.[34]

Our results allow also some specific mechanistic conclusions to be drawn, including the confirmation of the ease of formation and spin-trapping of tyrosyl radicals from reaction with Ce^{4+}, Ir^{4+} as well as ferryl-oxo species from enzymes. The relative ease of oxidation of tyrosine residues by the transition-metal ions studied becomes understandable in terms of their relatively low redox potentials for one-electron transfer and the stability (*via* delocalisation) of the tyrosyl phenoxyl radical. Thiyl-group oxidation may be anticipated and occurs readily in denatured proteins and with peroxynitrite. The predominance of attack at oxygen evidently reflects the number and the accessibility of phenolic oxygen atoms and, we believe, the difficulty in attack of oxidant on the buried thiyl moiety. Radical transfer (*via* electron- or hydrogen-transfer) from oxygen to sulfur has been demonstrated for different enzymes.[35] However, in our studies, experiments conducted with different trap concentrations and with O- or S-blocked proteins did not provide conclusive evidence for such transfer. Also notable is the facility with which the nitrones employed trap (stabilised) phenoxyl radicals; this is not simply a reaction imposed by the protein's environment since the same behaviour is shown by tyrosine itself in experiments with DMPO and DEPMPO.[21]

The formation of thiyl radical by reaction of peroxynitrite in its anionic form (O=NOO$^-$) with BSA has been demonstrated to be a one-electron oxidation. The formation of the hydroxyl free radical from decomposition of the neutral form of peroxynitrous acid (O=NOOH) or by reaction with the thiyl moiety does not appear to be significant under the conditions employed.

Finally further evidence is obtained for the formation of aliphatic carbon-centred protein-derived radicals (rather than phenoxyl or thiyl species) in reaction with $HO^{\bullet}$. The primary target for this relatively unselective radical is believed to be the C–H bond adjacent to a carboxy group.

Acknowledgements

This paper is dedicated to the late Professor Lennart Eberson in recognition of his outstanding contribution to research in physical organic chemistry. This work has been supported by the European Community (Marie Curie Fellowship to Jean-Louis Clément). The authors would also like to thank the Hungarian Scientific Fund OTKA T-032929 for financial support, Mlle Sandrine Lambert for her kind synthesis of DEPMPO, and Drs Adrian Whitwood and Yves Berchadsky for helpful discussions.

References

1 B. Halliwell, *Pathol. Biol.*, 1996, **44**, 6; G. Ambrosio and M. Chiarello, *Am. J. Med.*, 1991, **91**, 3c86s; M. J. Davies, *Free Radical Res. Commun.*, 1989, **7**, 275; S. Pietri, M. Culcasi and J. Cozzone, *Eur. J. Biochem.*, 1989, **186**, 163; *Oxygen Radicals and the Disease Process*, Ed. C. E. Thomas and B. Kalyanaraman, Harwood Academic Publisher, 1998.
2 B. Halliwell and J. M. C. Gutteridge, *Free Radical in Biology and Medicine*, 2nd Edn., Clarendon Press, Oxford, 1989, and references therein.
3 B. Halliwell and J. M. C. Gutteridge, *Methods Enzymol.*, 1990, **186**, 1 and references therein.
4 R. T. Dean, S. Fu, R. Stocker and M. J. Davies, *Biochem. J.*, 1997, **324**, 1.
5 M. J. Davies and R. T. Dean, *Radical-mediated protein oxidation: from chemistry to medicine*, Oxford University Press, Oxford, 1997; W. M. Garrison, *Chem. Rev.*, 1987, **87**, 381.
6 M. J. Davies, *Res. Chem. Intermed.*, 1993, **19**, 669.
7 M. J. Davies, B. C. Gilbert and R. M. Haywood, *Free Radical Res. Commun.*, 1991, **15**, 111.
8 S. H. Jeong and S. J. Hong, *J. Biochem. Mol. Biol.*, 1995, **28**, 293.
9 M. J. Davies, B. C. Gilbert and R. M. Haywood, *Free Radical Res. Commun.*, 1993, **18**, 353.
10 S. Barbati, J.-L. Clément, G. Olive, V. Roubaud, B. Tuccio and P. Tordo, *Free Radical Biol. Environ.*, Ed. F. Minisci, NATO ASI series, Series A Life Science, 1997, 27, 39; R. Lauricella, C. Fréjaville, J. C. Bouteiller and P. Tordo, *J. Chem. Soc., Perkin Trans. 2*, 1995, 295; C. Fréjaville, H. Karoui, F. Lemoigne, S. Pietri, M. Culcasi and P. Tordo, Fr. Pat. PV 9308906 of 20/07/93; C. Fréjaville, H. Karoui, B. Tuccio, F. Lemoigne, S. Pietri, M. Culcasi, R. Lauricella and P. Tordo, *J. Med. Chem.*, 1995, **38**, 258; C. Fréjaville, H. Karoui, B. Tuccio, F. Lemoigne, S. Pietri, M. Culcasi, R. Lauricella and P. Tordo, *J. Chem. Soc., Chem. Commun.*, 1994, 1793.
11 A. Rockenbauer and L. Korecz, *Appl. Magn. Reson.*, 1996, **10**, 29.
12 A. Rockenbauer, *Mol. Phys. Rep.*, 1999, **26**, 117.
13 P. Theodore, *Adv. Protein Chem.*, 1985, **37**, 161.
14 C. C. Blake, D. F. Koenig, G. A. Mair, A. C. North, D. C. Phillips and V. R. Sarma, *Nature*, 1965, **206**, 757.

15 S. Barbati, J.-L. Clément, C. Fréjaville, J. C. Bouteiller, J. C. Michel, J. C. Yadam and P. Tordo, *Synthesis*, 1999, **12**, 2036.
16 H. Karoui, N. Hogg, C. Fréjaville, P. Tordo and B. Kalyanaraman, *J. Biol. Chem.*, 1996, **271**, 6000.
17 G. E. Means and R. E. Feeney, *Chemical Modification of Protein*, Holden-Day Inc., San Francisco, 1971; R. E. Feeney, R. B. Yamasaki and K. F. Geoghegan, *Adv. Chem. Ser.*, 1982, **198**, 3; F. H. White, *Methods Enzymol.*, 1972, **25B**, 387; A. N. Glazer, R. J. Delange and D. S. Sigman, *Lab. Tech. Biochem. Mol. Biol.*, 1975, **4**, 68.
18 A. F. Habeeb, *Methods Enzymol.*, 1972, **25B**, 457.
19 A. Rockenbauer and P. Simon, *J. Magn. Reson.*, 1975, **18**, 320.
20 H. Miki, K. Harada, I. Yamazaki, M. Tamura and H. Watanabe, *Arch. Biochem. Biophys.*, 1989, **275**, 354.
21 M. R. Gunther, R. A. Tschirret-Guth, H. E. Witkowska, Y. C. Fann, D. P. Barr, P. R. Ortiz de Montellano and R. P. Mason, *Biochem. J.*, 1998, **330**, 1293; M. R. Gunther, B. E. Sturgeon and R. P. Mason, *Free Radical Biol. Med.*, 2000, **28**, 709.
22 K. R. Maples, S. J. Jordan and R. P. Mason, *Mol. Pharmacol.*, 1988, **33**, 344.
23 K. R. Maples, C. H. Kennedy, S. J. Jordan and R. P. Mason, *Arch. Biochem. Biophys.*, 1990, **277**, 402.
24 C. Chachaty, C. Mathieu, A. Mercier and P. Tordo, *Magn. Reson. Chem.*, 1998, **36**, 46.
25 G. R. Buettner, *Free Radical Biol. Mol.*, 1987, **3**, 259.
26 P. Graceffa, *Arch. Biochem. Biophys.*, 1983, **225**, 802.
27 W. Wolf, J. C. Kertesz and W. C. Landgraf, *J. Magn. Reson.*, 1969, **1**, 618.
28 D. J. Kelman, J. A. DeGray and R. P. Mason, *J. Biol. Chem.*, 1994, **269**, 7458.
29 H. Ostdal, H. J. Andersen and M. J. Davies, *Arch. Biochem. Biophys.*, 1999, **362**, 105.
30 R. M. Gatti, R. Radi and O. Augusto, *FEBS Lett.*, 1994, **348**, 287; J. Vasquez-Vivar, A. M. Santos, V. B. C. Junquiera and O. Augusto, *Biochem. J.*, 1996, **314**, 869; B. Alvarez, G. Ferrer-Sueta, B. C. Freeman and R. Radi, *J. Biol. Chem.*, 1999, **274**, 842.
31 J. S. Beckman, J. W Beckman, J. Chen, P. A. Marshall and B. Freeman, *Proc. Natl. Acad. Sci. U.S.A.*, 1990, **91**, 11173.
32 J.-L. Clément, B. C. Gilbert, P. Tordo and A. C. Whitwood, manuscript in preparation.
33 J.-L. Clément, PhD thesis, Université de St Jérôme, Marseille, 1998.
34 J.-L. Clément, B. C. Gilbert, P. Tordo and A. C. Whitwood, manuscript in preparation.
35 J. Stubbe and W. A. van der Donk, *Chem. Rev.*, 1998, **98**, 705.